RESEARCH ARTICLE

A Novel Benzene Structured Array Configuration for Harnessing Maximum Power From PV Array Under Partial Shading Condition With Reduced Number of Cross Ties

CHIDURALA SAIPRAKASH[ID][1], **(Student Member, IEEE)**,
ALIVARANI MOHAPATRA[ID][1], **(Member, IEEE), BYAMAKESH NAYAK**[ID][1],
THANIKANTI SUDHAKAR BABU[ID][2], **(Senior Member, IEEE)**,
AND HASSAN HAES ALHELOU[ID][3], **(Senior Member, IEEE)**

[1]School of Electrical Engineering, KIIT Deemed to be University, Bhubaneswar 751024, India
[2]Department of Electrical and Electronics Engineering, Chaitanya Bharathi Institute of Technology, Hyderabad 500075, India
[3]Department of Electrical Power Engineering, Faculty of Mechanical and Electrical Engineering, Tishreen University, Lattakia, Syria

Corresponding authors: Hassan Haes Alhelou (alhelou@ieee.org) and Alivarani Mohapatra (aliva.priti@gmail.com)

ABSTRACT Partial shading (PS) phenomena significantly degrade the power output from the photovoltaic (PV) array. Due to the PS effect, there is a mismatch in current between the PV modules of a series-connected PV string. As a result, in-shaded module power dissipates, resulting in increased module temperature and the creation of local hotspots. To avoid the hotspot effect, bypass diodes are connected anti-parallel to the PV modules. But the activation of bypass diodes creates multiple peaks in I-V and P-V characteristics. The effect of PS can be reduced by using a suitable array configuration and the performance of the PV array gets improved. Among all the existing PV array configurations, the total cross-tied (TCT) configuration performs better under partial shading conditions (PSCs). But the disadvantage of TCT is that it has an enormous number of tie connections, creating complexity in an array configuration and, therefore, more cable losses. The main objective of this paper is to propose a novel array configuration named benzene (BZ) configuration, which eliminates the demerits of the TCT array configuration. Benzene configuration has improved performance with fewer tie connections compared to conventional tie-connected configurations such as TCT, bridge link (BL), and honeycomb (HC). The performance of the tie-connected array configurations is analyzed under different PSCs by considering the various performance parameters such as global maximum power (GMP), the voltage at maximum power (Vmp), current at maximum power (Imp), mismatch loss (ML), shading loss (SL), fill factor (FF) and performance ratio. It is observed that the proposed benzene array configuration gives better output performance, even having lower mismatch losses with a reduced amount of tie connections. Further, the effect of the bypass diode on a partially shaded PV string is investigated through MATLAB Simulation and experimental analysis.

INDEX TERMS PV array configurations, benzene array configuration, maximum output power, fill factor (FF), shading loss (SL), mismatch loss (ML), partial shading condition (PSC).

NOMENCLATURE

BZ	Benzene
k	Boltzmann constant
BL	Bridge link
I_{mp}	Current at maximum power (A)
N_s	Number of series-connected modules
I-V	Current-Voltage

a	Diode ideality factor
T	Diode junction temperature (°C)
I_o	Diode saturation current (A)
q	Electron charge of 1.602×10^{-19}C
I_{pv}	Module output current (A)
STC	Standard test condition
V_{mp}	Voltage at maximum power (V)
KCL	Kirchhoff current law
LMPP	Local maximum power point
α	Shading factor
P_{gmpp}	Maximum power at global MPP (W)
MPP	Maximum Power Point
TCT	Total cross-tied
PS	Partial shading
ML	Mismatch loss (W)
I_{sh}	Module leakage current (A)
N_p	Number of strings connected in parallel
V_{pv}	Module output voltage (V)
HC	Honeycomb
V_{oc}	Open circuit voltage (V)
P	parallel
P_m	Maximum available power (W)
PSC	Partial shading condition
I_{ph}	Photo generated current (A)
I_{pho}	Photo-generated current at STC (A)
PV	Photovoltaic
n_s	Number of series cells in a module
I_d	Current flowing through the diode (A)
FF	Fill Factor
S	series
R_s	Series resistant (Ω)
MPPT	Maximum power point tracking
SL	Shading loss (W)
I_{sc}	Short circuit current (A)
R_p	Shunt resistant (Ω)
P-V	Power-Voltage
V_T	Thermal voltage
GMPP	Global Maximum Power Point

I. INTRODUCTION

The proliferation of the human population and industries, technological advancement, and livelihood modernization has led to increasing energy demand for human activities. In modern times, fossil fuels provide most of the world's energy. But the limited availability of fossil fuel resources and their harmful environmental impact necessitates renewable energy as an alternative energy source. Despite all other renewable sources, the solar photovoltaic (PV) system has emerged as the most convenient one due to its wide availability, free of cost, and eco-friendly nature [1]. Although it has disadvantages like low conversion efficiency and dependency on atmospheric conditions, it is still popularly used for its advantages, as mentioned above [2].

The partial shading condition (PSC) predominantly affects the solar PV system. Partial shadowing of PV arrays is
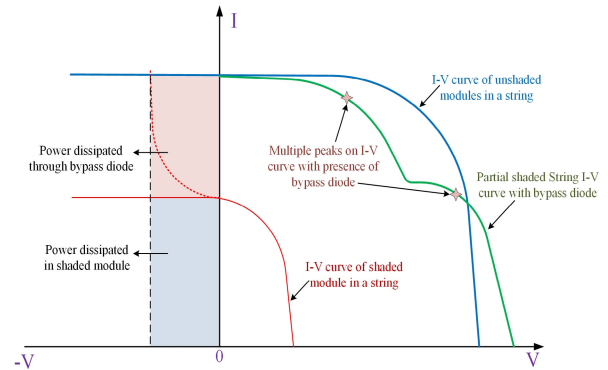

FIGURE 1. I-V characteristics of a PV string with bypass diode under PSC.

typically caused by shadows cast by shifting clouds, trees, nearby buildings, dust or dirt on PV modules, and bird droppings [3]. Under Partial shading conditions, some of the PV modules of a PV series string do not receive uniform irradiance. Due to this, a mismatch in current flow between the shaded and unshaded modules in the PV series string occurs. Under mismatch conditions, the shaded module operates in a reverse-biased region to match the current value of the unshaded modules [4]. FIGURE 1 shows how the shaded module operates in a reverse-biased region to match the current of the unshaded module. Under shading conditions, the shaded module in the series string behaves more like a load than a source. As a result, powers generated from the unshaded modules are dissipated through the shaded module. Due to this, a rise in temperature occurs in the shaded module and hotspot heating occurs in it [5]. Hotspot heating in modules may lead to cracks and damage the module. To overcome the hotspot effect, bypass diodes are configured in anti-parallel to the modules, as discussed in [6] and [7].

In a series string of modules, the connections of bypass diodes are always parallel with modules with opposite polarity. The bypass diode of the shaded module allows the string current from the unshaded modules to flow through when shading occurs in any of the modules in the series string. But due to the presence of a bypass diode, multiple peaks affect the I-V and P-V characteristics curve [8], [9]. Among multiple peaks, one is a global peak, and the others are local peaks. Multiple peaks create difficulty in designing the maximum power point tracking (MPPT) algorithm [10]. Therefore to mitigate the partial shading (PS) effect and to improve the performance of the PV system, suitable array configurations and proper MPPT controllers are required [4], [11]. The cause of PS effects on PV array and their mitigation techniques to get the maximum output power from the PV array is illustrated in FIGURE 2.

There are several array configurations presented by the literature, including the series (S), parallel (P), series-parallel (SP), bridge link (BL), honeycomb and Total cross tie (TCT), configurations [12], [13], [14]. In a series configuration, modules are connected as a series string. In a series configuration, an equal amount of current flows through all the modules in
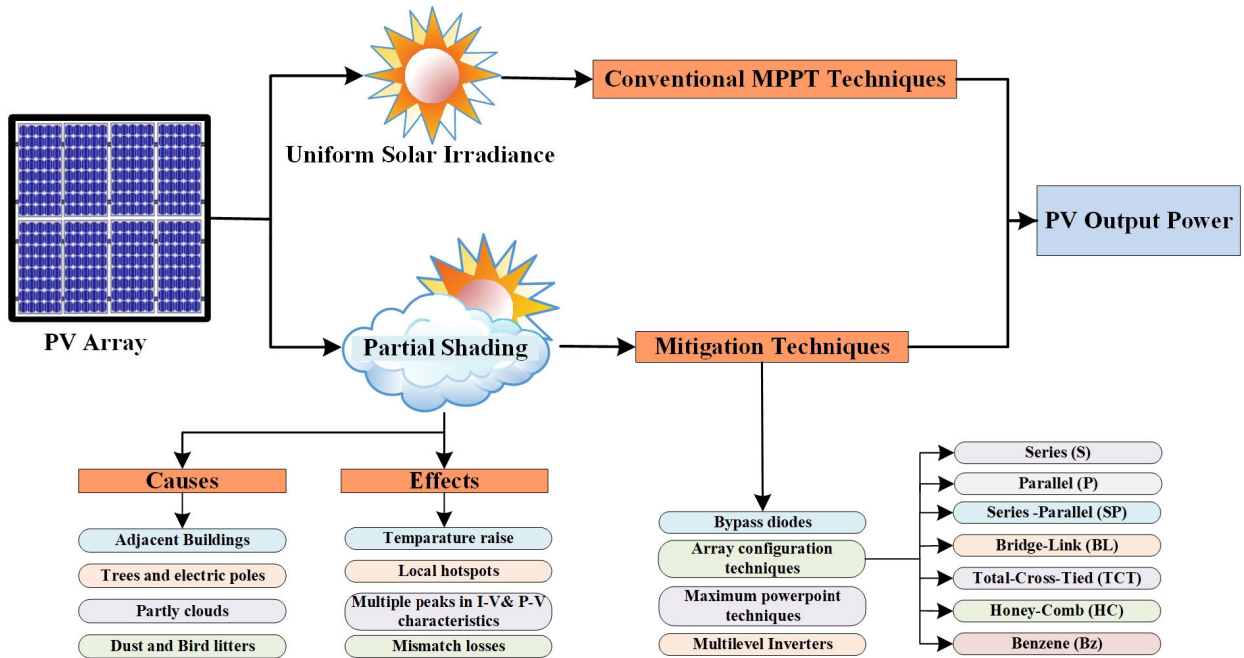
the string and the array voltage is equal to the total sum of the module's string voltages.

If shading occurs on any module in the series string, there is a current mismatch in the entire string, and the output power decreases [15], [16]. In a parallel array configuration, modules are connected parallel to each other; therefore, there is no chance of a current mismatch. In a parallel configuration, the output array voltage is the same as the individual module voltage, while the output current is the sum of parallel-connected modules' current [17]. As the output current is less in a series array configuration and the output voltage is less in a parallel array configuration; therefore series (S) and parallel (P) configurations are combined to form a series-parallel (SP) array configuration to acquire the desired amount of voltage and current at its output from the PV system [18].

Modules are first connected in series to create a series string, which is followed by the parallel connection of series strings to create the SP array. SP configuration is the basic conventional array configuration. But the presence of more series strings in the SP array makes it prone to current mismatch while operating under PSC [19]. Therefore, the performance of the SP configuration is less under the PSC. To minimize current mismatch, different array configurations are introduced in the literature, such as Honeycomb (HC), Bridge Link (BL), and Total cross-tied (TCT) array configurations [20]. For interconnection configurations, tie connections are present between the SP configuration's parallel strings. Due to intertie connections, the number of series-connected modules is reduced in a series string. As a result, mismatch losses are reduced and the performance of the PV array got increased in interconnected array configurations [21], [22].

In the TCT array configuration, cross ties are coupled in each row junction of the SP configuration. Because of the presence of cross-tie connections, each module in an array is interconnected with others and there is less chance of conduction of bypass diodes. Therefore mismatch losses and occurrence of multiple peaks are less under PSC for TCT, and it gives a higher performance compared to SP array configuration [23]. But due to more interconnection in TCT, cable losses are and even it is hard to detect the faulty module under fault conditions. To reduce cable losses and array complexity, the number of interconnections is decreased in the BL and honeycomb array configuration [24].

In BL array design, the number of cross-tie links is cut in half compared to TCT. Although BL has fewer tie connections, BL configurations give less output power under PSC [20]. By increasing the number of ties in the configuration, the BL array is changed to the HC array to increase the performance under PSC [13]. To further improve the performance of PV array under PSC, hybrid array configurations are introduced by combining the conventional structure as BL-TCT, BL-HC, HC-TCT, and SP-TCT as discussed in [25] and [26]. Although these hybrid array arrangements perform better than conventional array configurations, there are more tie connections in the hybrid structures than in the traditional setups [27].

To enhance the performance of PV arrays with fewer tie connections, a novel array design known as the benzene (BZ) structured array arrangement has been presented in this paper. In comparison to modified PV array configurations like TCT, BL, and HC, the BZ array has fewer tie connections but offers better output performance.
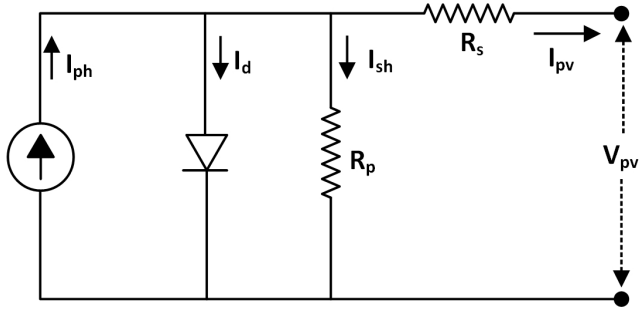
FIGURE 3. Equivalent circuit model of a photovoltaic module.

FIGURE 4. Equivalent circuit of a PV array.

II. MATHEMATICAL MODELLING
A. MATHEMATICAL MODELING OF PV MODULE
The equivalent circuit of the PV module can be represented with the single diode in parallel to the photo-generated current, as shown in FIGURE 3. By applying the KCL, the PV module's output current is stated as an equation (1) [28]

$$I_{pv} = I_{ph} - I_d - I_{sh} \tag{1}$$

I_{pv} is the module output current, I_{ph} is the photo-generated current of the PV module, I_d is the current flowing through the diode, and it is expressed as the equation (2).

$$I_d = I_o \left[\exp\left(\frac{V_{pv} + I_{pv}R_s}{n_s V_T a} \right) - 1 \right] \tag{2}$$

where, I_o is the diode saturation current, n_s denotes the number of series cells in the module, V_{pv} is the module output voltage, a is the ideality factor of the diode, R_s and R_{sh} are equivalent series and shunt resistances and it can be calculated using equation (3).

$$V_T = \frac{kT}{q} \tag{3}$$

where, k is the Boltzmann constant having the value of 1.3807×10.23 J/K, T represents the junction temperature of the diode in Kevin, and q is the electron charge having the value of 1.602×10.19 C. The leakage current of the PV module is written as an equation (4).

$$I_{sh} = \frac{V_{pv} + I_{pv}R_s}{R_{sh}} \tag{4}$$

From the equation(1), (2) and (4), the output current of a PV module is stated as an equation (5) [28].

$$I_{pv} = I_{ph} - I_0 \left[\exp\left(\frac{V_{pv} + I_{pv}R_s}{n_s V_T a} \right) - 1 \right] - \frac{V_{pv} + I_{pv}R_s}{R_p} \tag{5}$$

B. MATHEMATICAL MODELLING OF PV ARRAY
PV modules are coupled in series (S), parallel (P), and series-parallel (S-P) configurations to make the array that fulfills the high-power demand. PV array is an interconnection system of PV modules. In a PV array, PV modules are connected in series to form the series string, and string-connected modules are connected in parallel to create the array. The equivalent
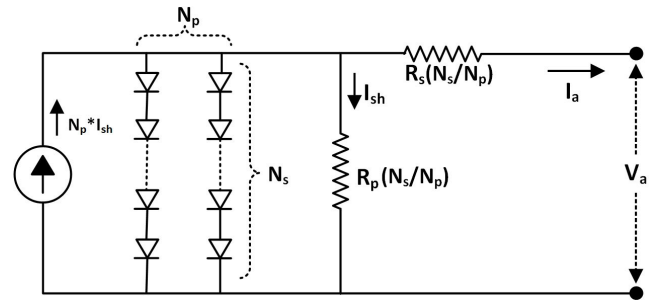
circuit of a PV array is shown in FIGURE 4. The PV array output current is expressed as the equation(6)[29].

$$I_a = N_p I_{ph} - N_p I_0 \left[\exp\left(\frac{V_a + (N_s/N_p)I_a R_s}{N_s V_T a} \right) - 1 \right] - \frac{V_a + (N_s/N_p)I_a R_s}{(N_s/N_p)R_p} \tag{6}$$

III. EXPERIMENTAL ANALYSIS OF THE EFFECT OF BYPASS DIODE ON PARTIAL SHADED PV STRING
If the shaded module operates for a long time in a reverse-biased region, the temperature rises and reaches the break-down voltage due to power dissipation. As a result, the hotspot effect occurs and damages the shaded PV module. To overcome the hotspot effect, bypass diodes are connected anti-parallel to the PV modules. Due to the presence of bypass diodes, there is an occurrence of multiple peaks happens in the I-V and P-V characteristics of the PV array. The multiple peak effect due to the bypass diode under partial shading conditions is analyzed through simulation and experimental setup, and these are shown in FIGURE 5, FIGURE 6, FIGURE 7, and FIGURE 8.

Two series-connected PV modules are taken into consideration with and without bypass diodes, as shown in FIGURE 5(a) and FIGURE 5(b), respectively, to examine the impact of bypass diodes in PV strings. The KC200GT PV module specifications were used for analysis through simulation for series-connected PV modules, including and excluding bypass diodes. The KC200GT PV module parameters are shown in Table 1. Under uniform irradiance conditions, PV modules are operated at their rated voltages and generate the global maximum power of 390.33W, as shown in FIGURE 5(c). From the obtained results, it is observed that under uniform irradiance conditions, the output power of the PV array is the same with and without the bypass diode, as shown in FIGURE 5(c).

Under shading condition, PV module 1(M1) and module 2(M2) receives irradiance of 1000 W/m² and 600 W/m² as shown in FIGURE 6(a) and FIGURE 6(b), respectively. When bypass diodes are not connected to the modules, as shown in FIGURE 6(a), the M2 will operate under a reversed biased region to match the string current, resulting in a hotspot. Bypass diodes are connected

TABLE 1. KC200GT PV module parameters at STC[30].

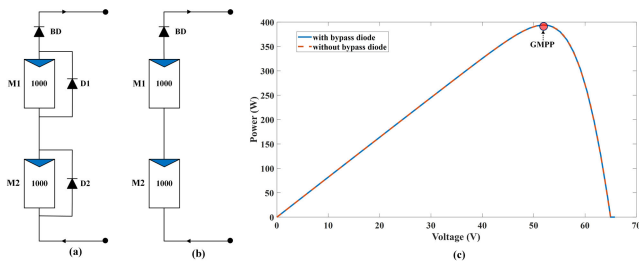| Parameter	Value
Maximum power of the module, P_{max}	200.13W
Open circuit voltage, V_{oc}	32.9 V
Voltage at MPP, V_{mp}	26.4 V
Current at MPP, I_{mp}	7.58 A
Short circuit current, I_{sc}	8.21 A
Temperature coefficient of voltage, K_v	-0.1230 V/K
Temperature coefficient of current, K_i	0.0032 A/K
No. of cells connected in series, N_s	54

FIGURE 5. Series connected PV string with and without bypass diodes under uniform irradiance (a) PV string with bypass diodes (D1,D2), (b) PV string without bypass diode, (c) P-V curves.

with the modules to avoid hotspot formation, as shown in FIGURE 6(b). The bypass diode connected in the module provides an alternate path to current flow resulting in the creation of various power crests in the power-voltage (P-V) characteristics curve as LMPP and GMPP, as shown in FIGURE 6(c). Without a bypass diode under shading conditions, the power output is less compared to the conduction of the bypass diode, as shown in FIGURE 6(c).

An experimental setup is developed to verify the simulation results as presented in FIGURE 9. The set up associated with two series-connected PV modules of Eldora 40 make and two regulated lamps, which are used to illuminate the PV modules with variable irradiance. It has a voltage, current, and temperature measuring unit. For the analysis of the effect of the bypass diode, modules are connected with and without the bypass diode. The pot meter is used as a variable resistive load. A polythene color sheet is covered on PV the module to create artificial shading conditions. To record the measured values of current and voltages, the Data logger and plotter box is connected to the output of the measuring unit. The recorded data from the logger plotter box is plotted through the ECOSENSE real-time plotter by connecting to the personal computer. The plotted P-V curves are shown in FIGURE 7 and FIGURE 8 with and without bypass diodes respectively. From the obtained P-V curves, it is observed that under shading conditions, multiple peaks occur with the bypass diode. Without a bypass diode, the temperature of the shaded module got increased and degraded the output power.
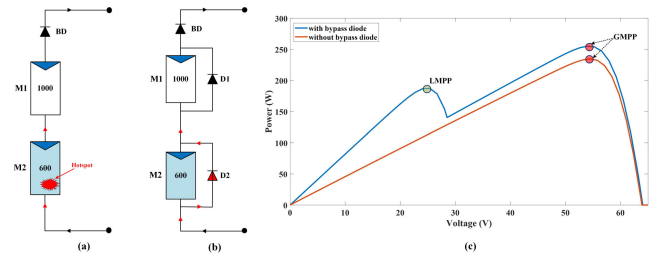

FIGURE 6. Series connected PV string with and without bypass diodes under partial shading (a) PV string without bypass diodes, (b) PV string with bypass diodes (D1 and D2 conduct under partial shading), (c) P-V curves.
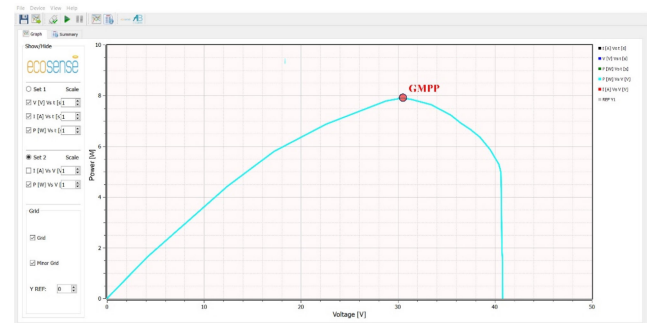

FIGURE 7. Experimental P-V curves of PV string under PSC without bypass diodes.
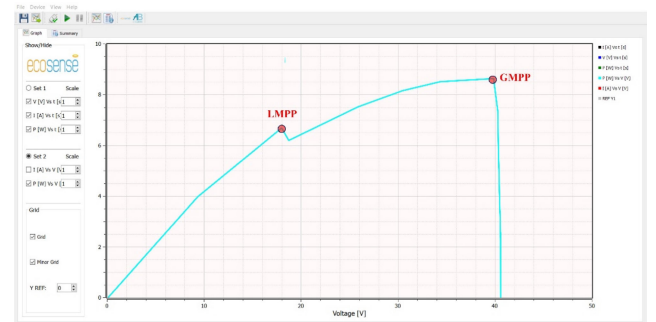

FIGURE 8. Experimental P-V curves of a PV string under PSC with bypass diodes.

IV. CONVENTIONAL PV ARRAY CONFIGURATIONS

In PV systems, solar modules are wired in series or in parallel to get the desired output power. In string-connected PV string, the loss is more due to current mismatch and more mismatch loss under the shading condition. The limitation of a parallel-connected PV array is that it operates at low voltage and high current, which needs proper power conditioning. To overcome the demerits of series and parallel connected PV arrays, PV modules are coupled in the SP fashion to get the desired output current and voltage. The primary SP and its derived array configurations are HC, BL, and TCT.

Among conventional array configurations, the SP configuration as shown in FIGURE 10(a), is the most economical and widely used configuration. But under PSC, SP configuration gives lower performance due to the presence of large series
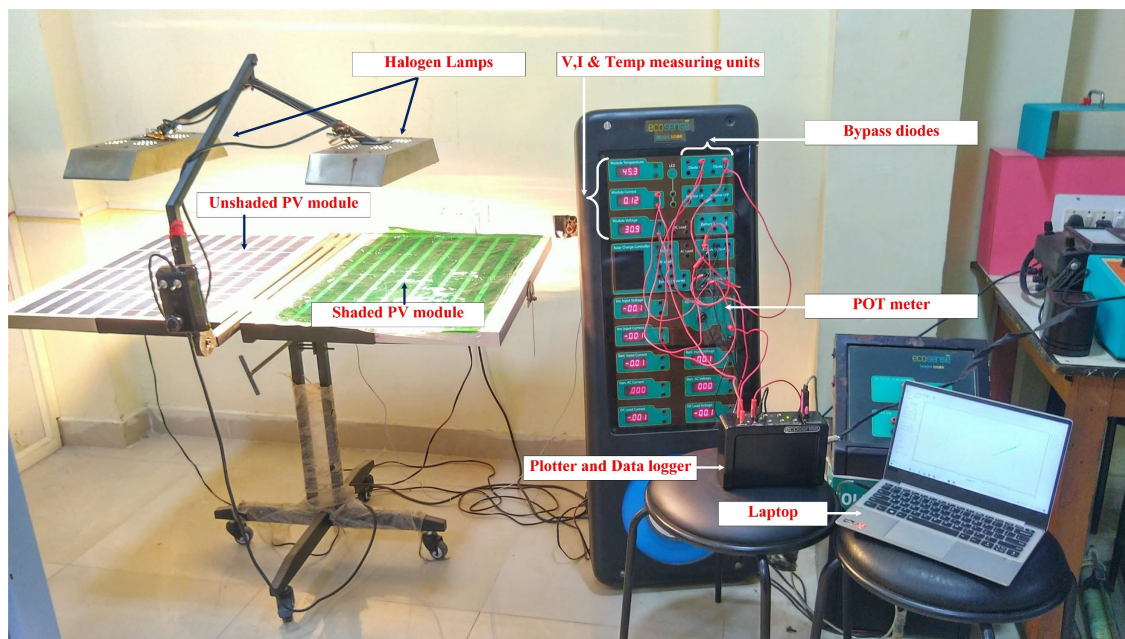
FIGURE 9. An experimental setup consisting of two ELDORA-40 PV module connected in series.

strings. To reduce the size of the series strings, tie connections are added to SP configurations and derived array configurations such as HC, BL, and TCT configurations come into the picture [20].

TCT array configurations as depicted in FIGURE 10(b), have many cross-ties across each series string of the module's junction. Due to large interconnection, initial cost, cable losses are more and detection of fault is also difficult.

In BL configuration, as shown in FIGURE 10(c), the tie connections are connected to the SP configuration in a bridge rectifier way. Each 2×2 sub-array is treated as one bridge unit, and each bridge is connected with cross ties. The BL array configuration has decreased performance under the PSC. It is modified as an HC configuration to overcome the drawbacks of BL array configuration [12]. HC configuration is shown in FIGURE 10(d). The HC array configuration is inspired by the honey bees' house structure. A honeycomb structure is created by placing the cross ties between the SP configuration series strings to form the HC configuration. The HC array configuration performs better than the SP and BL configurations with more tie connections [13].

V. PROPOSED PV ARRAY CONFIGURATION

The proposed configuration is inspired by the chemical compound Benzene (BZ) structure as shown in FIGURE 11(a). Benzene is an organic hydrocarbon molecule; it has six hydrogen and six carbon atoms, and its chemical formula is C_6H_6. In this structure, six carbon atoms make a ring, and each carbon atom makes a single bond with a hydrogen atom, as shown in FIGURE 11(b). The benzene cluster is configured as an array formation and is shown in FIGURE 11(c). In the proposed array configuration, the modules are placed

TABLE 2. Comparison of the number of tie connections present for different PV array configurations.

Array size	Array configurations			
	TCT	HC	BL	BZ
5X5	16	10	10	**9**
6X6	25	13	12	**11**
7X7	36	18	18	**18**
8X8	49	24	24	**20**

between the carbon atoms i.e., at the sides of the hexagon. The bonding between the carbon and hydrogen atom is taken as the tie connection as shown in FIGURE 11(d). The simplified 6×6 Benzene array configuration is represented as shown in FIGURE 11(e).

The main advantages of the proposed benzene structured array configuration are greater performance and fewer tie connections than the conventional tie array configuration. The cable cost for the proposed array configuration is smaller since there are fewer tie connections present in it. The numbers of tie connections present in different array configurations with varying sizes of the array are compared in Table 2. Table 2 demonstrates that as the array size increases, the tie connection significantly decreases, which lowers the cost of the array.

VI. ANALYSIS OF PARTIAL SHADING CONDITION

Ten distinct shading situations have been considered to examine the effectiveness of the various tie-linked array topologies. These shading conditions are categorized as columns, rows, and diagonal patterns shown in FIGURE 12. For analysis
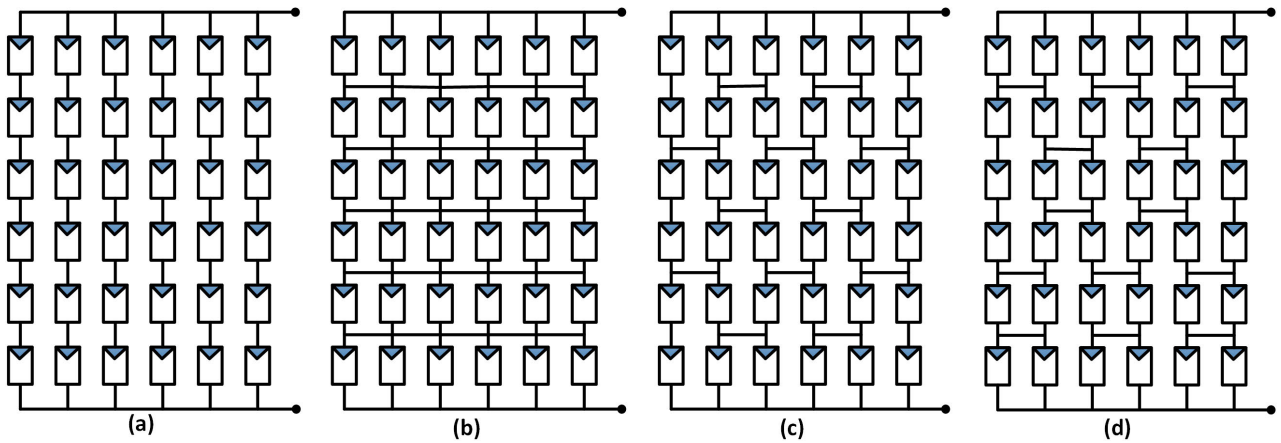
FIGURE 10. Conventional PV array configurations (a) SP, (b) TCT, (c) BL and (d) HC.
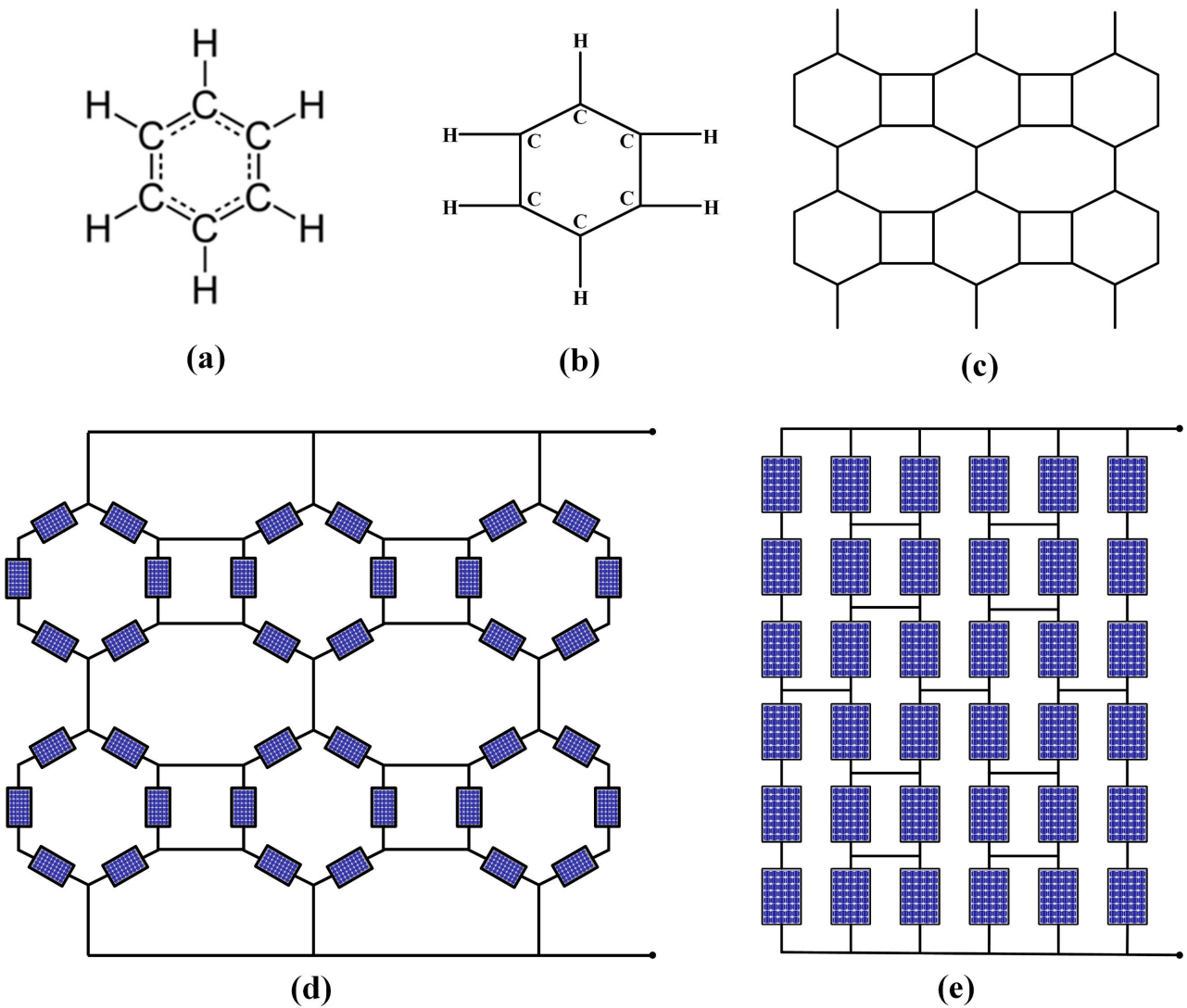

FIGURE 11. Proposed benzene array configuration. (a) Benzene structure, (b) Benzene ring structure, (c) configured cluster of benzene structures, (d) Modules arranged, (e) simplified benzene structured 6 × 6 array configuration.

purpose, a 6 × 6 PV array has been considered in which modules are shaded with different irradiance levels. Modules are exposed to different irradiance levels of 1000 W/m², 700 W/m², and 500 W/m² by keeping the temperature
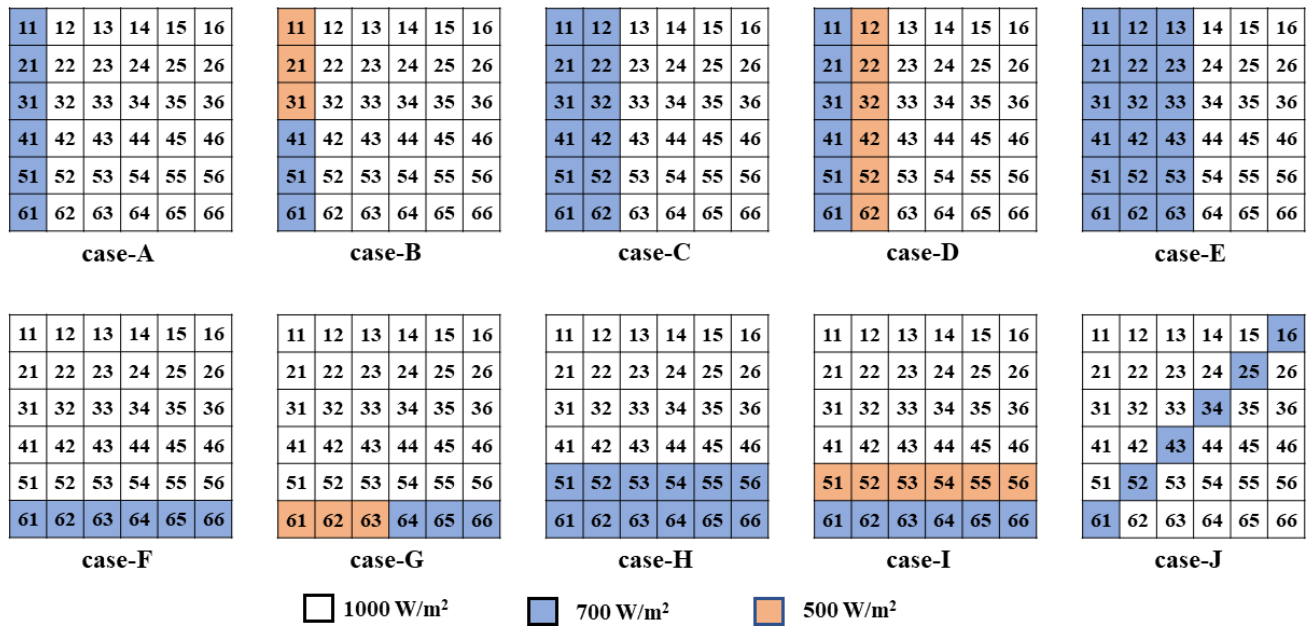
FIGURE 12. Different Partial shading conditions, column wise(case-A to case-E), row wise (case-F to case-I), diagonal shading (case-J).

constant at 25°C. Shading case-A to case-E as column pattern and row pattern is from case-F to case-I. Case-J is called a diagonal pattern. For the performance analysis, all the array configurations under different shading cases are simulated in MATLAB Simulink by considering the KC200GT PV modules. The parameter values of the KC200GT PV module are shown in Table 1.

VII. RESULTS AND DISCUSSIONS

The performance of the proposed BZ array configuration is analyzed under various shading situations to determine the global maximum power, mismatch loss, shading loss, performance ratio, and Fill factor. The obtained PV characteristics curves of the different array configurations under considered shading conditions are shown in FIGURE 13. From the PV characteristic curves, values for the global peak power (Pgmpp), current at peak power (Imp), and voltage at peak power (Vmp) were gathered and tabulated in Table 4.

Through observation of PV characteristics, all array configurations under uniform insolation conditions generate an equal amount of global maximum power of 7164.979 W. As opposed to TCT, BL, and HC topologies, the proposed benzene (BZ) PV array configuration has the highest maximum power of 6796.616 W in case-A shading condition. In shading case-B, the BZ array structure provides the peak power of 6631.650 W with improved efficiency than the HC and BL topologies. In the shading case-C, peak power yields from the BZ topology is 6427.981 W, which proves superiority over HC, TCT and BL array structure. In shading case-D, the BZ configuration generates a higher maximum power of 6177.945 W in comparison to the conventional PV array configurations. In shading case-E situations, the

peak power of 6063.768 W is generated from the BZ array topology, which is higher than the power generated from traditional topologies. The highest power from the BZ configuration is 5925.764 W in case-F shading conditions, which is comparable to the TCT array arrangement and greater than BL and HC topologies. The BZ topology produces a peak power of 5925.038 W in shading case-G and is comparable to the HC and TCT configurations and greater than the BL configuration. For shading case-H, the BZ arrangement provides the highest maximum power of 5530.919 W and is comparable to the TCT, BL, and HC configurations. For the shading case-I pattern, BZ gives better results than the BL and yields a peak power of 4690.858 W. In the shading case-J condition, the performance of the BZ configuration proves superior to the HC and BL configurations, and it generates a maximum power of 6462.616 W. According to the obtained results, the proposed BZ array arrangement provides superior performance with less number of ties connections with reduced cost.

A. SHADING LOSS

Shading losses in solar PV arrays occur due to partial shading on PV modules. The difference between the amounts of maximum available power under STC to the sum of each module's available power under PSC gives the shading loss (SL) [31]. The shading loss is calculated using the equation(7).

$$Shading\ Loss(SL) = P_{\max,STC} - P_{\max,im} \qquad (7)$$

Here, $P_{max,\ STC}$ is the array's maximum power under standard test conditions, and $P_{max,\ im}$ is the sum of individual available power under partial shading conditions. Under STC, the available maximum power for the considered PV array
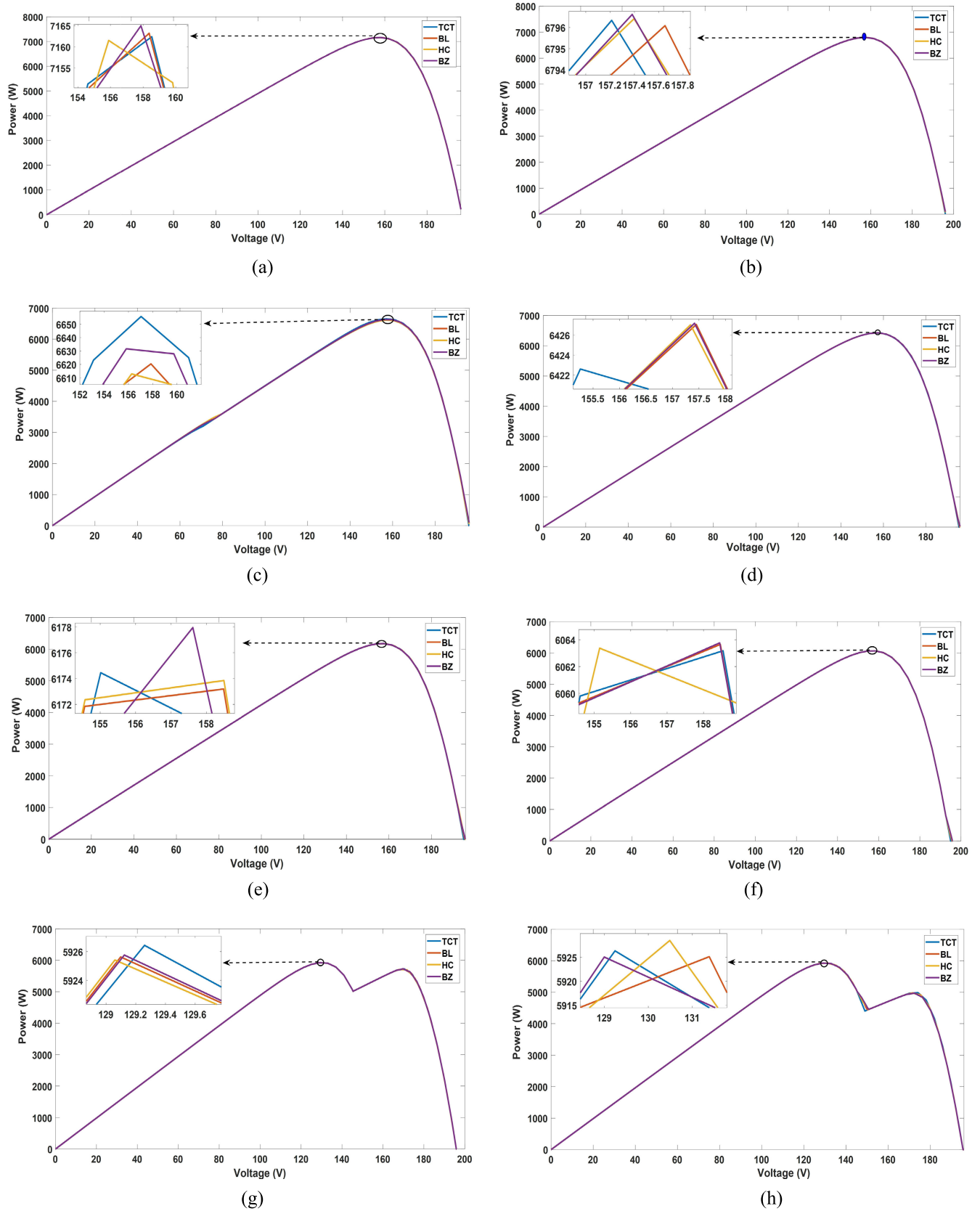
FIGURE 13. P-V characteristics curves of different array configurations under shading conditions (a) uniform, (b) case- A, (c) case-B, (d) case- C, (e) case-D, (f) case-E, (g) case-F, (h) case-G, (i) case-H, (j) case-I, (k) case-J.

FIGURE 13. (Continued.) P-V characteristics curves of different array configurations under shading conditions (a) uniform, (b) case-A, (c) case-B, (d) case-C, (e) case-D, (f) case-E, (g) case-F, (h) case-G, (i) case-H, (j) case-I, (k) case-J.
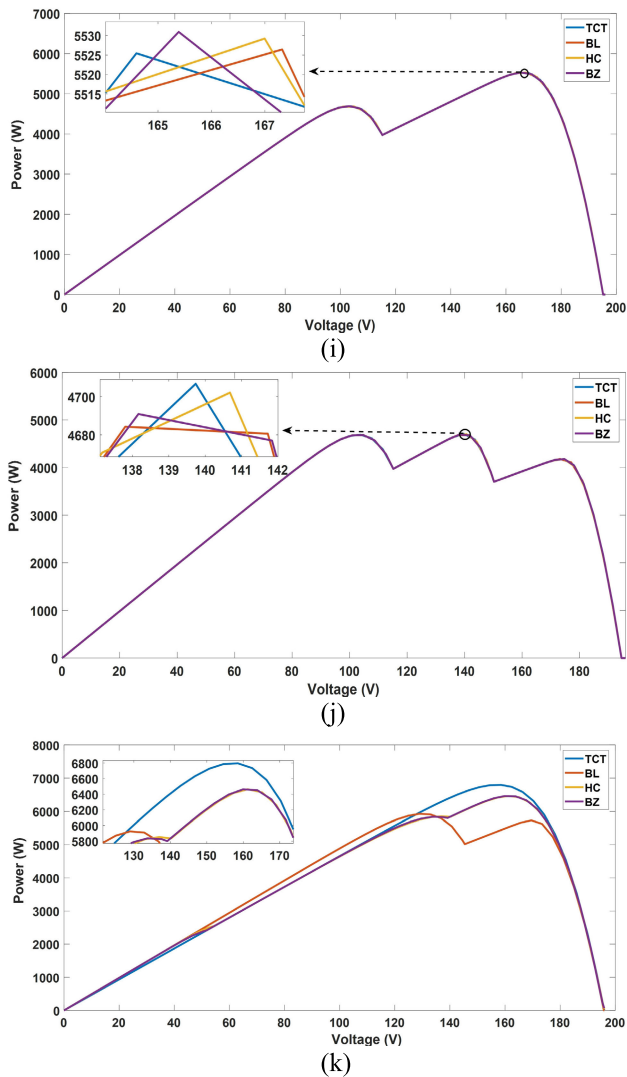
TABLE 3. The sum of individual available maximum power under different shading conditions.

Shading cases	$\sum P_{max,im}$
case-A	6832.98
case-B	6709.26
case-C	6465.96
case-D	6218.52
case-E	6098.94
case-F	6832.98
case-G	6709.26
case-H	6465.96
case-I	6218.52
case-J	6832.98
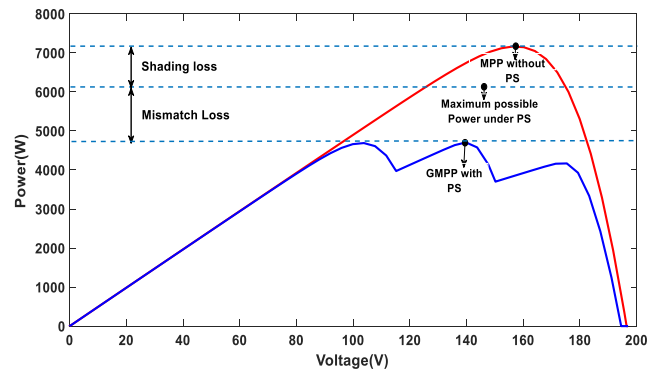
FIGURE 14. Representation of mismatch and shading loss resulting from partial shading.

configuration is 7164.98W. Table 3 lists the sum of the individual available maximum power under different shading conditions. The calculated shading loss values for the considered array configurations are tabulated in Table 5. The shading loss for case-A, case-F, and case-J are the same and calculated as 332.006W, in which six modules are shaded with an equal amount of irradiance with different shading patterns. For case-B and case-G, modules are shaded with an equal amount of irradiance with different patterns and the calculated shading loss is 455.726W. For case-C and case-H, shading loss is the same and its value is 699.026W.

Similarly, case-D and case-I have the same shading loss value of 946.466W with different shading patterns. Shading loss for case-E is significantly high and calculated as 1066.046, from which it is observed that the shading loss mainly depends on the intensity of irradiance received by the PV modules of an array irrespective of the shading pattern.

The shading losses for all array configurations for ten shading cases are graphically represented in FIGURE 15.

B. MISMATCH LOSS

Mismatch losses are occurred in PV array configurations under PSC due to the current mismatch in the PV series string. The performance of the PV array configuration is analyzed by calculating the mismatch losses [32]. Mismatch loss is calculated using the equation (8). Shading loss is inherently there in the PV system if the PV array is exposed to PSC. Mismatch loss can be minimized by intelligent selection of PV array configurations. The difference between the shading and mismatch loss is clearly visualized as shown in FIGURE 14.

$$Mismatch\ loss(ML) = P_{\max,im} - P_{gmpp\max,ps} \qquad (8)$$

where, $P_{max,im}$ is defined for the equation(7), and $P_{gmpp,ps}$ is the generated global maximum power under PSC. The calculated ML values for the entire PV array configurations under studied shading cases are tabulated in Table 6. The following conclusions can be drawn from the findings that mismatch losses (MLs) are less in the column-wise shading condition (i.e., case-A to case-E), in which shade is concentrated on particular strings only. Mismatch losses are more in row-wise shading conditions (i.e., case-F to case-I) and diagonal shading conditions (i.e., case-J), in which shade

TABLE 4. Maximum power generated by the PV array under various shading conditions.

Shading condition	parameters	configurations			
		TCT	BL	HC	BZ
uniform	V_{mpp} (V)	157.86	157.86	157.86	157.86
	I_{mpp} (I)	45.388	45.388	45.388	45.388
	P_{mpp} (W)	7164.979	7164.979	7164.979	7164.979
case-A	V_{mpp} (V)	157.213	157.652	157.397	157.382
	I_{mpp} (I)	43.23	43.108	43.18	43.186
	P_{mpp} (W)	6796.318	6796.078	6796.415	6796.616
case-B	V_{mpp} (V)	157.039	157.854	156.264	155.819
	I_{mpp} (I)	42.383	41.94	42.319	42.56
	P_{mpp} (W)	6655.721	6620.407	6612.932	6631.65
case-C	V_{mpp} (V)	155.259	157.45	157.341	157.416
	I_{mpp} (I)	41.367	40.82	40.852	40.829
	P_{mpp} (W)	6422.623	6427.078	6427.643	6427.981
case-D	V_{mpp} (V)	155.014	158.483	158.491	157.615
	I_{mpp} (I)	39.832	38.952	38.954	39.196
	P_{mpp} (W)	6174.452	6173.194	6173.842	6177.945
case-E	V_{mpp} (V)	158.536	158.461	155.149	158.443
	I_{mpp} (I)	38.245	38.266	39.081	38.271
	P_{mpp} (W)	6063.182	6063.645	6063.378	6063.768
case-F	V_{mpp} (V)	129.259	129.099	129.06	129.123
	I_{mpp} (I)	45.849	45.9	45.912	45.892
	P_{mpp} (W)	5926.439	5925.63	5925.415	5925.764
case-G	V_{mpp} (V)	129.244	131.383	130.487	129.586
	I_{mpp} (I)	45.854	45.098	45.434	45.931
	P_{mpp} (W)	5926.341	5925.115	5928.494	5925.038
case-H	V_{mpp} (V)	164.596	167.324	166.996	165.387
	I_{mpp} (I)	33.57	33.028	33.11	33.442
	P_{mpp} (W)	5525.448	5526.434	5529.207	5530.919
case-I	V_{mpp} (V)	139.738	104.797	140.681	138.163
	I_{mpp} (I)	33.682	44.68	33.424	33.952
	P_{mpp} (W)	4706.684	4682.357	4702.087	4690.858
case-J	V_{mpp} (V)	158.533	128.932	161.224	159.922
	I_{mpp} (I)	42.868	48.953	40.087	40.411
	P_{mpp} (W)	6795.981	6311.674	6462.91	6462.616

is distributed among all strings. From the obtained results, it is observed that ML is 25 times more in case-F compared

to case-A, but the intensity of irradiance received by the modules for both cases is identical, but the distribution of

TABLE 5. shading loss(W) of PV array configurations under various partial shading conditions.

Configuration	case-A	case-B	case-C	case-D	case-E	case-F	case-G	case-H	case-I	case-J
TCT	332.006	455.726	699.026	946.466	1066.046	332.006	455.726	699.026	946.466	332.006
BL	332.006	455.726	699.026	946.466	1066.046	332.006	455.726	699.026	946.466	332.006
HC	332.006	455.726	699.026	946.466	1066.046	332.006	455.726	699.026	946.466	332.006
Benzene	332.006	455.726	699.026	946.466	1066.046	332.006	455.726	699.026	946.466	332.006

TABLE 6. Mismatch loss(W) of PV array configurations under various partial shading conditions.

Configuration	case-A	case-B	case-C	case-D	case-E	case-F	case-G	case-H	case-I	case-J
TCT	36.646	**53.532**	43.343	44.070	35.763	**906.538**	782.924	940.513	**1511.832**	**307.001**
BL	36.896	88.858	38.891	45.332	35.289	907.346	784.141	939.532	1536.158	908.308
HC	36.570	96.324	**38.323**	44.672	35.569	907.560	**780.762**	936.755	1516.437	370.076
Benzene	**36.367**	77.610	38.770	**40.568**	**35.176**	907.216	784.215	**935.046**	1514.656	370.359

TABLE 7. Fill factor of PV array configurations under various partial shading conditions.

configuration	Uniform	case-A	case-B	case-C	case-D	case-E	case-F	case-G	case-H	case-I	case-J
TCT	0.7366	0.6989	0.6845	0.6605	0.6350	0.6235	0.6095	0.6095	0.5682	0.4840	0.6989
BL	0.7367	0.6989	0.6808	0.6610	0.6348	0.6236	0.6094	0.6093	0.5683	0.4815	0.6093
HC	0.7365	0.6989	0.6801	0.6610	0.6349	0.6236	0.6094	0.6097	0.5686	0.4836	0.6646
Benzene	0.7368	0.6990	0.6820	0.6610	0.6353	0.6236	0.6094	0.6093	0.5688	0.4824	0.6645

TABLE 8. Performance ratio of PV array configurations under various partial shading conditions.

configuration	case-A	case-B	case-C	case-D	case-E	case-F	case-G	case-H	case-I	case-J
TCT	94.855	92.892	89.639	86.175	84.622	82.714	82.712	77.117	65.690	94.850
BL	94.851	92.399	89.701	86.158	84.629	82.703	82.695	77.131	65.351	82.689
HC	94.856	92.295	89.709	86.167	84.625	82.700	82.743	77.170	65.626	90.201
Benzene	94.859	92.556	89.703	86.224	84.631	82.704	82.694	77.194	65.469	90.183

shade among the strings is different. From this, it is concluded that MLs are more whenever the shade is distributed on more stings in a PV array. Mismatch losses can be minimized with proper PV array design and location for various shading circumstances.

Table 6 further shows that for most shading scenarios, MLs are lower in the BZ array arrangement than in all other array topologies. Compared to the HC, BL, and TCT configurations, the ML for the BZ configuration is the lowest at 36.367 W for the shadowing condition in pattern A. For the shading condition of case B, TCT has the lowest ML of 53.532 W, and BZ has the second-lowest value of 77.610W, which is lower than the BL and HC array configurations. BZ has the lowest ML of 38.770 W and 40.568 W, respectively, for case-C and case-D shading conditions. In case-E shading, all configurations have a similar mismatch loss in which BZ has the lowest ML of 35.176 W. In case-F, the BZ configuration gives the lowest ML of 907.216 W after TCT has the value of 906.538W. For shading case-G, the proposed BZ array configuration gives similar performance to other configurations having an ML of 784.215 W. In the case-H shading scenario, the BZ array gives the lowest ML

of 935.046 W. In case-I shading, ML for BZ configuration is 1514.656W and has improved results than HC and BL array structure. When there is case-J shading, the BL configuration has a maximum ML of 908.308W and it is two times more than that of the proposed BZ array configuration, which has an ML of 370.359W. For the proposed BZ array configuration, MLs are lowest compared to the other configuration giving better performance even having less number of tie connections. Mismatch loss for all PV array configurations under different shading conditions is graphically represented as shown in FIGURE 16.

C. FILL FACTOR
Fill factor (FF) is the ratio of the product of the PV system's maximum voltage and current to the product of the system's open-circuit voltage and short-circuit current, and it is denoted by the equation (9) [33]. FF indicates the efficiency of a PV module. The higher FF represents the better power conversion efficiency of the PV module.

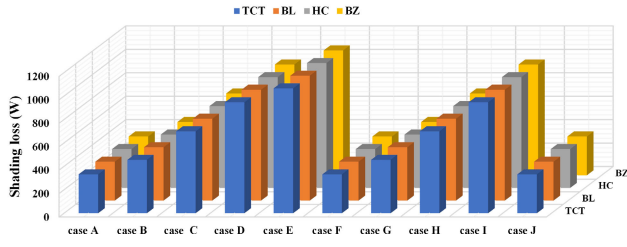$$Fill\ Factor(FF) = \frac{V_{max} * I_{max}}{V_{oc} * I_{sc}} \quad (9)$$

FIGURE 15. Shading loss of different array configurations under different shading cases.

Table 7 lists the FF values for various array configurations. The results show that the BZ array configuration provides better FF for column-wise shading conditions (i.e., case-A, case-B, case-D, and case-E) compared to TCT, BL, and HC configurations. For row and diagonal shading conditions, the BZ array configuration gives a better FF value compared to the BL array and nearly the same results as HC and TCT array configurations. For the studied shading conditions, the proposed BZ array gives better FF, even having fewer counts of tie connections. Fill factors of all array configurations under numerous shading conditions are graphically represented in FIGURE 17.

D. PERFORMANCE RATIO
The performance ratio is the ratio of the maximum power yield under PSC to the maximum accessible amount of power from the PV system and it is shown in equation (10) [34]. It represents the percentage of energy actually available after deducting energy losses. The calculated performance ratio values are tabulated in Table 8.

$$Performance\ Ratio\ (\%) = \frac{P_{m\ (available)}}{P_{m\ (reference)}} \times 100 \qquad (10)$$

Here, $P_{m(available)}$ is the maximum power yield under the PSC, and $P_{m(reference)}$ is the maximum accessible power from the PV array. The results show that the proposed BZ array configuration gives a better performance ratio for column-wise shading conditions (i.e., case-A, case-C, case-D, and case-E) in comparison to the BL, HC, and TCT configurations. For row-wise and diagonal shading conditions, the BZ array configuration gives a better performance ratio than the HC and BL array configuration and gives a good result as TCT array configurations. For the studied shading conditions, the proposed BZ array configuration provides a better performance ratio than the BL array topology despite having fewer tie connections. The performance ratio for all the array configurations under different shading cases is graphically represented in FIGURE 18.

VIII. COMPARATIVE STUDY
The proposed benzene array arrangement and discussed ties-connected array configurations, such as HC, BL, and TCT are compared in terms of their performance when a 6∗6 array size is taken into consideration. The performance is analyzed under uniform and various PSCs with respect to
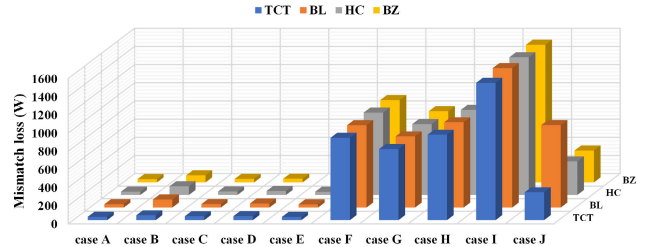

FIGURE 16. Mismatch loss of different array configurations under different shading cases.
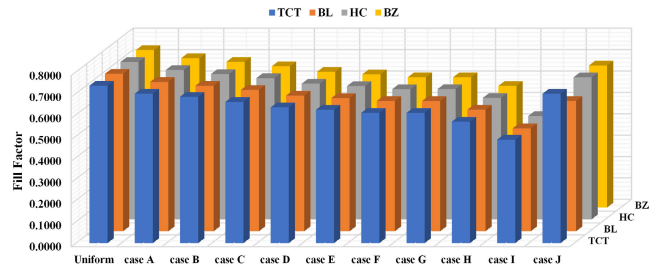

FIGURE 17. Fill factor of different array configurations under different shading cases.
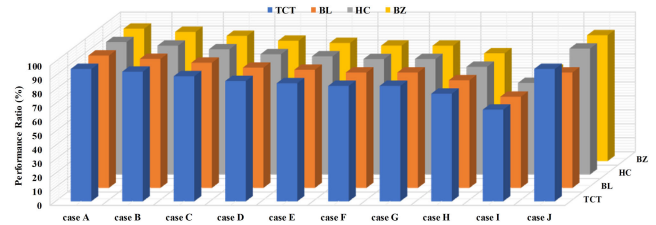

FIGURE 18. Performance ratio of different array configurations under different shading cases.

global maximum power, shading loss, fill factor (FF), power loss, and mismatch loss. Under uniform irradiance conditions, it is observed that all the PV array configurations generate the same amount of global maximum power (GMPP) of 7164.97 W, a fill factor of 0.74, and zero (0) mismatch power loss. In comparison to other PV array configurations, the BZ configuration produces the highest global peak power, lowest mismatch power losses, best performance ratio, and better Fill Factors (FF) under the column-wise shading condition. For row-wise and diagonal shading conditions, the BZ PV array configuration has proven to be the best next to TCT. Even with fewer crossed ties, BZ produces maximum power closer to that of TCT, hence reducing the cost of wiring and minimizing losses. In comparison, the TCT PV array configuration requires 25 cross-ties for the 6 × 6 array whereas the BZ PV array configuration requires only 11 crossed–ties. Despite having less than half of the number of cross–ties in comparison to TCT, BZ array configuration still provides comparable results with TCT. In addition, BZ array configuration provides better performance in comparison to BL and HC under different shading conditions despite having fewer tie connections, as given in Table.2

IX. CONCLUSION

The performance comparison of the proposed benzene (BZ) array configurations is evaluated with the other configurations such as TCT, BL, and HC. BZ has been modeled and simulated in MATLAB Simulink and the obtained results are compared with all conventional tie configurations. When compared to TCT, BL, and HC configurations, BZ has fewer tie connections; still, it gives better performances in most of the shading scenarios. The BZ configuration provides a higher peak power for column-wise shading cases than TCT, BL, and HC. For row-wise shading cases, BZ gives a comparable performance with the TCT and gives better results when compared to HC and BL. Mismatch losses and power losses are less in BZ even though it has fewer tie connections than the BL and HC configurations. The number of tie connections for large array sizes is reduced to more than half in the BZ configuration compared to the TCT configuration. The BZ array configuration is the most cost-effective, with fewer cable connections and better performance, justifying its superiority over other traditional array configurations. From the above discussion, the proposed Benzene (BZ) structured PV array configuration is the best choice for large PV arrays that experience partial shading frequently.

In addition, in this article, the effect of bypass diode under PSC has been analyzed through experimental and MATLAB simulation. From the experimental results, it is observed that without the usage of bypass diodes, module temperature rises and leads to permanent damage to the PV module. To avoid the hotspots effect, bypass diodes are always connected to the module, although it creates multiple peaks on P-V characteristics curves. For this reason, PV array configurations must be properly designed to reduce the effect of multiple peaks.

REFERENCES

[1] T. M. Razykov, C. S. Ferekides, D. Morel, E. Stefanakos, H. S. Ullal, and H. M. Upadhyaya, "Solar photovoltaic electricity: Current status and future prospects," *Sol. Energy*, vol. 85, no. 8, pp. 1580–1608, Aug. 2011, doi: 10.1016/j.solener.2010.12.002.

[2] B. Parida, S. Iniyan, and R. Goic, "A review of solar photovoltaic technologies," *Renew. Sustain. Energy Rev.*, vol. 15, pp. 1625–1636, Apr. 2011, doi: 10.1016/j.rser.2010.11.032.

[3] S. K. Das, D. Verma, S. Nema, and R. K. Nema, "Shading mitigation techniques: State-of-the-art in photovoltaic applications," *Renew. Sustain. Energy Rev.*, vol. 78, pp. 369–390, Oct. 2017, doi: 10.1016/j.rser.2017.04.093.

[4] A. Mohapatra, B. Nayak, P. Das, and K. B. Mohanty, "A review on MPPT techniques of PV system under partial shading condition," *Renew. Sustain. Energy Rev.*, vol. 80, pp. 854–867, Dec. 2017, doi: 10.1016/j.rser.2017.05.083.

[5] S. Ghosh, V. K. Yadav, and V. Mukherjee, "Improvement of partial shading resilience of PV array though modified bypass arrangement," *Renew. Energy*, vol. 143, pp. 1079–1093, Dec. 2019, doi: 10.1016/j.renene.2019.05.062.

[6] R. Vieira, F. de Araújo, M. Dhimish, and M. Guerra, "A comprehensive review on bypass diode application on photovoltaic modules," *Energies*, vol. 13, no. 10, p. 2472, May 2020, doi: 10.3390/en13102472.

[7] R. Ahmad, A. F. Murtaza, H. A. Sher, U. T. Shami, and S. Olalekan, "An analytical approach to study partial shading effects on PV array supported by literature," *Renew. Sustain. Energy Rev.*, vol. 74, pp. 721–732, Jul. 2017, doi: 10.1016/j.rser.2017.02.078.

[8] A. Mohapatra, B. Nayak, and K. B. Mohanty, "Analytical approach to locate multiple power peaks of photovoltaic array under partial shading condition and hybrid array configuration schemes to reduce mismatch losses," *Energy Sources, A, Recovery, Utilization, Environ. Effects*, pp. 1–22, Jul. 2021, doi: 10.1080/15567036.2021.1945710.

[9] M. Premkumar and R. Sowmya, "An effective maximum power point tracker for partially shaded solar photovoltaic systems," *Energy Rep.*, vol. 5, pp. 1445–1462, Nov. 2019.

[10] Z. Zhao, M. Zhang, Z. Zhang, Y. Wang, R. Cheng, J. Guo, P. Yang, C. S. Lai, P. Li, and L. L. Lai, "Hierarchical pigeon-inspired optimization-based MPPT method for photovoltaic systems under complex partial shading conditions," *IEEE Trans. Ind. Electron.*, vol. 69, no. 10, pp. 10129–10143, Oct. 2022, doi: 10.1109/TIE.2021.3137595.

[11] M. Abouelela, "Power electronics for practical implementation of PV MPPT," in *Modern Maximum Power Point Tracking Techniques for Photovoltaic Energy Systems*. Switzerland: Springer, 2020, pp. 65–105.

[12] S. R. Pendem and S. Mikkili, "Modeling, simulation and performance analysis of solar PV array configurations (series, series–parallel and honey-comb) to extract maximum power under partial shading conditions," *Energy Rep.*, vol. 4, pp. 274–287, Nov. 2018, doi: 10.1016/j.egyr.2018.03.003.

[13] Y.-J. Wang and P.-C. Hsu, "An investigation on partial shading of PV modules with different connection configurations of PV cells," *Energy*, vol. 36, no. 5, pp. 3069–3078, May 2011, doi: 10.1016/j.energy.2011.02.052.

[14] C. Saiprakash, A. Mohapatra, and B. Nayak, "An a TT array configuration for performance enhancement of PV system under PSC," in *Proc. 1st Int. Conf. Power Electron. Energy (ICPEE)*, Jan. 2021, doi: 10.1109/ICPEE50452.2021.9358645.

[15] S. Malathy and R. Ramaprabha, "Comprehensive analysis on the role of array size and configuration on energy yield of photovoltaic systems under shaded conditions," *Renew. Sustain. Energy Rev.*, vol. 49, pp. 672–679, Sep. 2015, doi: 10.1016/j.rser.2015.04.165.

[16] G. S. Krishna and T. Moger, "Comparative study on solar photovoltaic array configurations under irregular irradiance conditions," in *Proc. 8th IEEE India Int. Conf. Power Electron. (IICPE)*, Dec. 2018, pp. 1–6, doi: 10.1109/IICPE.2018.8709512.

[17] R. Ramabadran and B. Mathur, "Effect of shading on series and parallel connected solar PV modules," *Modern Appl. Sci.*, vol. 3, no. 10, p. 32, Sep. 2009.

[18] P. K. Bonthagorla and S. Mikkili, "A novel fixed PV array configuration for harvesting maximum power from shaded modules by reducing the number of cross-ties," *IEEE J. Emerg. Sel. Topics Power Electron.*, vol. 9, no. 2, pp. 2109–2121, Apr. 2021, doi: 10.1109/jestpe.2020.2979632.

[19] A. S. Yadav and V. Mukherjee, "Conventional and advanced PV array configurations to extract maximum power under partial shading conditions: A review," *Renew. Energy*, vol. 178, pp. 977–1005, Nov. 2021, doi: 10.1016/j.renene.2021.06.029.

[20] O. Bingöl and B. Özkaya, "Analysis and comparison of different PV array configurations under partial shading conditions," *Sol. Energy*, vol. 160, pp. 336–343, Jan. 2018, doi: 10.1016/j.solener.2017.12.004.

[21] S. Malathy and R. Ramaprabha, "Reconfiguration strategies to extract maximum power from photovoltaic array under partially shaded conditions," *Renew. Sustain. Energy Rev.*, vol. 81, pp. 2922–2934, Jan. 2018, doi: 10.1016/j.rser.2017.06.100.

[22] C. Saiprakash, A. Mohapatra, B. Nayak, and S. R. Ghatak, "Performance enhancement of PV array under partial shading condition by modified BL configuration," in *Proc. IEEE Calcutta Conf. (CALCON)*, Feb. 2020, pp. 308–312, doi: 10.1109/CALCON49167.2020.9106517.

[23] S. Mohammadnejad, A. Khalafi, and S. M. Ahmadi, "Mathematical analysis of total-cross-tied photovoltaic array under partial shading condition and its comparison with other configurations," *Sol. Energy*, vol. 133, pp. 501–511, Aug. 2016, doi: 10.1016/j.solener.2016.03.058.

[24] F. M. Aboshady and I. B. M. Taha, "Fault detection and classification scheme for PV system using array power and cross-strings differential currents," *IEEE Access*, vol. 9, pp. 112655–112669, 2021, doi: 10.1109/ACCESS.2021.3104007.

[25] N. Mishra, A. S. Yadav, R. Pachauri, Y. K. Chauhan, and V. K. Yadav, "Performance enhancement of PV system using proposed array topologies under various shadow patterns," *Sol. Energy*, vol. 157, pp. 641–656, Nov. 2017, doi: 10.1016/j.solener.2017.08.021.

[26] A. S. Yadav, R. K. Pachauri, Y. K. Chauhan, S. Choudhury, and R. Singh, "Performance enhancement of partially shaded PV array using novel shade dispersion effect on magic-square puzzle configuration," *Sol. Energy*, vol. 144, pp. 780–797, Mar. 2017, doi: 10.1016/j.solener.2017.01.011.

[27] Manjunath, H. N. Suresh, and S. Rajanna, "Performance enhancement of hybrid interconnected solar photovoltaic array using shade dispersion magic square puzzle pattern technique under partial shading conditions," *Sol. Energy*, vol. 194, pp. 602–617, Dec. 2019, doi: 10.1016/j.solener.2019.10.068.

[28] A. Mohapatra, B. Nayak, and B. Misra, "Model validation and maximum power point tracking of photovoltaic module," in *Proc. Power Energy Syst., Towards Sustain. Energy*, Mar. 2014, pp. 1–4, doi: 10.1109/PESTSE.2014.6805314.

[29] B. Dhanalakshmi and N. Rajasekar, "Dominance square based array reconfiguration scheme for power loss reduction in solar photovoltaic (PV) systems," *Energy Convers. Manage.*, vol. 156, pp. 84–102, Jan. 2018, doi: 10.1016/j.enconman.2017.10.080.

[30] K. Yadav and B. Kumar, "Mitigation of mismatch power losses of PV array under partial shading condition using novel odd even configuration," *Energy Rep.*, vol. 6, pp. 427–437, Nov. 2020, doi: 10.1016/j.egyr.2020.01.012.

[31] G. Meerimatha and B. L. Rao, "Novel reconfiguration approach to reduce line losses of the photovoltaic array under various shading conditions," *Energy*, vol. 196, Apr. 2020, Art. no. 117120, doi: 10.1016/j.energy.2020.117120.

[32] P. R. Satpathy and R. Sharma, "Power and mismatch losses mitigation by a fixed electrical reconfiguration technique for partially shaded photovoltaic arrays," *Energy Convers. Manage.*, vol. 192, pp. 52–70, Jul. 2019, doi: 10.1016/j.enconman.2019.04.039.

[33] G. S. Krishna and T. Moger, "Enhancement of maximum power output through reconfiguration techniques under non-uniform irradiance conditions," *Energy*, vol. 187, Nov. 2019, Art. no. 115917, doi: 10.1016/j.energy.2019.115917.

[34] P. R. Satpathy, P. Bhowmik, T. S. Babu, C. Sain, R. Sharma, and H. H. Alhelou, "Performance and reliability improvement of partially shaded PV arrays by one-time electrical reconfiguration," *IEEE Access*, vol. 10, pp. 46911–46935, 2022, doi: 10.1109/ACCESS.2022.3171107.

CHIDURALA SAIPRAKASH (Student Member, IEEE) received the B.Tech. degree in electrical and electronics engineering and the M.Tech. degree in power electronics from Jawaharlal Nehru Technological University, Hyderabad, India, in 2011 and 2015, respectively. He is currently pursuing the Ph.D. degree in renewable energy engineering with KIIT Deemed to be University, Bhubaneswar, India. He was worked as a Graduate Engineer at Rural Electrification Corporation Ltd., (REC Ltd., India) and he has about three years of experience in electrical installation, maintenance, and commissioning. He has published several international conferences and journal articles. His research interests include power systems, renewable energy systems, design and implementation of solar PV systems, PV system fault detection, efficiency improvement of PV array, and power system protection. He is an Associate Member of the Institute of Engineers, India.

ALIVARANI MOHAPATRA (Member, IEEE) received the B.Tech. degree in electrical engineering from Utkal University, Bhubaneswar, India, the master's degree in electrical engineering from the Birla Institute of Technology, Mesra, Ranchi, India, and the Ph.D. degree in electrical engineering from the National Institute of Technology, Rourkela, India. She has more than 18 years of experience in teaching and research. Currently, she is currently working as an Assistant Professor with the School of Electrical Engineering; KIIT Deemed to be University, Bhubaneswar. Her research interests include modeling, analysis, and control of photovoltaic energy systems. She is a Life Member of ISTE and a member of the Institution of Engineers (India). She is serving as a Reviewer in various reputed journals, such as IEEE Transactions on Sustainable Energy, IEEE Access, Elsevier, Wiley, and Taylor & Francis.

BYAMAKESH NAYAK received the master's degree from the Institute of Technology, Banaras Hindu University, Banaras, India, and the Ph.D. degree from the Kalinga Institute of Industrial Technology (KIIT) Deemed to be University, Bhubaneswar, both in electrical engineering. He is currently working as a Professor and the Dean of the School of Electrical Engineering, KIIT Deemed to be University. He has 20 years of teaching and research experience. He has vast knowledge of electrical engineering with industry experience. His research interests include power electronics and electrical drives, hybrid electric vehicle, renewable energy, and application of PIC microcontrollers in special drive applications. He is serving as a Reviewer in various prestigious journals, such as IEEE Transactions on Industrial Informatics, IEEE, IET, Elsevier, and Taylor & Francis.

THANIKANTI SUDHAKAR BABU (Senior Member, IEEE) received the B.Tech. degree from Jawaharlal Nehru Technological University, Ananthapur, India, in 2009, the M.Tech. degree in power electronics and industrial drives from Anna University, Chennai, India, in 2011, and the Ph.D. degree from VIT University, Vellore, India, in 2017. He worked as a Post-Doctoral Researcher with the Department of Electrical Power Engineering, Institute of Power Engineering, University Tenaga Nasional (UNITEN), Malaysia. He is currently working as an Associate professor with the Department of IEEE, Chaitanya Bharathi Institute of Technology, Hyderabad, India. He has published more than 130 research articles in various renowned international journals. His research interests include design and implementation of solar PV systems, renewable energy resources, power management for hybrid energy systems, storage systems, fuel cell technologies, electric vehicle, and smart grid. He has been acting as an Editorial Board Member and a Reviewer for various reputed journals, such as the IEEE Access, IEEE, IET, Elsevier, and Taylor & Francis.

HASSAN HAES ALHELOU (Senior Member, IEEE) is currently a Faculty Member at Tishreen University, Lattakia, Syria. He was a Ph.D. Researcher at the Isfahan University of Technology (IUT), Isfahan, Iran. He is included in the 2018 and 2019 Publons list of the top 1% best reviewer and researchers in the field of engineering. He was a recipient of the Outstanding Reviewer Award from *Energy Conversion and Management* journal, in 2016, *ISA Transactions* journal, in 2018, *Applied Energy* journal, in 2019, and many other awards. He was a recipient of the Best Young Researcher in the Arab Student Forum Creative among 61 researchers from 16 countries at Alexandria University, Egypt, in 2011. He has published more than 30 research papers in the high quality peer-reviewed journals and international conferences. He has also performed more than 160 reviews for high prestigious journals, including IEEE Transactions on Industrial Informatics, IEEE Transactions on Industrial Electronics, *Energy Conversion and Management*, *Applied Energy*, and *International Journal of Electrical Power & Energy Systems*. He has participated in more than 15 industrial projects. His major research interests include power systems, power system dynamics, power system operation and control, dynamic state estimation, frequency control, smart grids, micro-grids, demand response, load shedding, and power system protection.

● ● ●